Iran J Sci Technol Trans Civ Eng
https://doi.org/10.1007/s40996-017-0082-z

RESEARCH PAPER

Shear Demands of Steel Moment-Resisting Frames Under Near- and Far-Fault Seismic Excitations

Morteza Razi[1] · Mohsen Gerami[1] · Reza Vahdani[1]

Received: 16 September 2016 / Accepted: 27 October 2017
© Shiraz University 2017

Abstract
Strength capacity checking and instability control of building structures require the prediction of story shear demands and other actions produced by seismic excitations. Impulsive feature and large vertical accelerations associated with near-fault ground motions may lead to instability of the structural systems with severe damaging outcomes. The seismic demands depend on structural and ground motion characteristics. In this paper, the effect of ground motion impulsive characteristics on the story shear demands of steel moment frames is investigated for different hazard levels. For this purpose, incremental dynamic analysis is conducted on five steel frames with 3–15 stories subjected to different types of ground motions. Moreover, the accuracy of conventional pushover and static linear procedures is examined and some modification factors are suggested for each analytical approach. Finally, the effect of vertical component of near-fault records is investigated for two case studies. The results of the study demonstrate that story shear demands obtained from static procedures must be amplified for stories located at the upper one-third of the structure by a modification factor of up to 2.5 to find more precise shear demands, depending on parameters such as structure height, story level, analysis method and ground motion type. Among pushover cases, the first-mode load pattern gives more reliable results compared to other load patterns. Also, it was found that the application of vertical component of long-period pulse-like accelerograms increases the column axial forces by up to 100%.

Keywords Shear demand · Near-fault ground motions · Steel moment frame · Seismic evaluation · Nonlinear response

1 Introduction

There are various analytical methods to evaluate the seismic demands of different types of structures for design purposes and other practices. In spite of the ongoing developments in new complicated analytical approaches (e.g., adaptive pushover analysis, incremental dynamic analysis and time-endurance analysis methods) which offer more precise estimations for the seismic response of structures, the conventional static procedures are currently the most frequent approaches for analyzing and designing building new structures (ASCE 07-10; Iranian seismic design code) as well as the seismic assessment of existing structures (FEMA 356; ASCE 41-13). This is due to the simplicity and applicability of these methods in modeling, analyzing and processing the results. For this reason, the improvement in static procedures' accuracy is a necessity for the structural engineering community.

According to the Iranian code for seismic design of structures, the application of static analysis method is valid for a wide range of structures which satisfy the regularity requirements and some other limiting specifications. In this method, the design base shear is calculated based on the dynamic behavior characteristics of equivalent single-degree-of-freedom system. The base shear is then distributed along the height of structure in the form of pseudolateral forces. Seismic response quantities are then calculated using the static analysis methods. Therefore, the pattern of lateral force distribution over the height of structure as well

✉ Reza Vahdani
rvahdani@semnan.ac.ir

Morteza Razi
m.razi@students.semnan.ac.ir

Mohsen Gerami
mgerami@semnan.ac.ir

[1] Department of Civil Engineering, Semnan University, Semnan 3513119111, Iran

Published online: 04 December 2017

as the estimation of base shear demand significantly influences the seismic response evaluations.

The primary criteria for design of steel frames, especially mid- and high-rise frames, are limiting the story drift ratio (IDR) demands to prescribed values. According to the fourth edition of Iranian seismic design code for structures with 5 stories or less, the maximum IDR of all stories considering the second-order geometric nonlinearity must be limited to the 0.025. This limit is 0.02 for buildings with more than five stories. Besides the limiting lateral displacements to prescribed values, the strength capacity of the elements must sufficiently satisfy the capacity design specifications to ensure the stability of individual members. In other words, each structural member must be designed to resist internal force/moment actions.

To control the structural stability of each story, instability index is defined as:

$$\theta_i = \frac{P_{\mathrm{ui}}\Delta_{\mathrm{eu}}}{V_{\mathrm{ui}}h}. \tag{1}$$

where P_{ui} is the sum of gravity loads in the ith to nth stories, Δ_{eu} is the relative displacement of the story, V_{ui} is the story shear demand, and h is the story height. This ratio must not exceed $\theta_{\max}$ which is calculated from Eq. (2).

$$\theta_{\max} = \frac{0.65}{C_{\mathrm{d}}} \leq 0.25 \tag{2}$$

In this equation, C_{d} is the displacement amplification factor which is proposed as 5.5 for special steel moment-resisting frames. This yields 0.118 for $\theta_{\max} = \theta_{\max}$. Story shear demands and increase in vertical loads due to vertical component of ground motion records as well as the structural properties influence the instability index.

Third edition of Iranian seismic design code (2005) suggests the following equation to estimate the lateral force distribution over the height of the building structures:

$$F_i = \frac{w_i h_i}{\sum_{j=1}^{n} w_j h_i}(V - F_{\mathrm{t}}) \tag{3}$$

where w is the seismic weight of story, h is the story height, i is the story number, and n is the number of total stories. F_{t} is a fraction of the total base shear equal to $0.07VT$ for $T > 0.7$ s and equal to zero for shorter periods, where T is the fundamental period of vibration. For the roof level, the F_{t} is added to lateral forces obtained from Eq. (3). This parameter is included to account for the higher-mode effects.

The fourth edition of Standard No. 2800 (2015) provides a different expression for lateral force distribution as presented in Eq. (4).

$$F_i = \frac{w_i h_i^k}{\sum_{j=1}^{n} w_j h_j^k} V \tag{4}$$

where k is a function of the fundamental period of oscillation as follows:

$$k = 0.75 + 0.5T \quad \text{and} \quad 1 < k < 2 \tag{5}$$

This equation is the same as the one presented in FEMA 356 and ASCE 7-10 standards for static analysis of the building structures. This relationship tends to represent the shape of fundamental mode of vibration. Eurocode 8 (2004) suggests that the lateral story forces are proportional to the product of story seismic mass by story displacement associated with the first mode of vibration.

According to the aforementioned statements, the pattern of lateral force distribution, which directly results in story shear demands, is essentially computed based on the linear elastic characteristics of the structures. Regarding the fact that the seismic response of common structural systems subjected to severe ground motions is expected to be highly nonlinear, the change in story relative stiffness due to the formation of plastic hinges within the structural elements may alter the shear distribution pattern. Some researchers proposed modification factors to estimate the story and base shear demands for different intensities (Medina and Krawinkler 2005; Pattinga and Priestley 2005). They concluded that the shear demands of the structures mainly depend on the structural properties (e.g., relative story stiffness), frequency content of the ground motion record and earthquake intensity. Kumar et al. (2013) investigated the shear demands of steel moment frames designed to specifications of Eurocode 8 under far-fault motions. They concluded that the shear demands depend on frequency content of the motion. Accordingly, the critical pulse period range depends on the ground motion intensity. Also, they found that shear distribution pattern obtained from static analysis with first-mode load pattern would result in unconservative shear demands for upper stories. Therefore, some modification factors were suggested to calibrate the shear demands. In another research, Gerami and Abdollahzadeh (2015) conducted a series of time-history analyses on the steel moment frames imposed to near-fault excitations and concluded that near-fault motions induce more shear demands but do not severely influence the pattern of shear distribution over the height. However, the effect of pulse period and nonlinearity level was not scrutinized. This paper investigates the effect of short- and long-period excitations on shear demands of steel moment-resisting frames, considering different hazard levels. The results obtained for pulse-like excitations are compared with standard far-fault motions. Regarding the fact that relative story stiffness of the buildings depends on the design specifications and the philosophy adopted in the

design process, the predictive models developed for certain types of structures may not be justified to expand for constructions design with different specifications. The focus of this study is on the SMRF structures designed in compliance with fourth edition of Iranian seismic design code.

Incremental dynamic analysis is utilized to evaluate the seismic response parameters under two sets of pulse-like near-fault records as well as far-fault ordinary ground motions. Results obtained from time-history analyses are compared with linear and nonlinear static procedures. Seismic design codes suggest the same pattern for all kinds of ground motions in different nonlinearity states. The accuracy of this method is examined here.

In addition to impulsive effects of near-fault excitations on the seismic shear demands, the vertical component of near-fault motions may produce significant internal actions, particularly in column members. The results of previous studies have shown that the axial force demand of columns in moment frame buildings may be increased by 80% due to application of seismic vertical loads (Sultana and Youssef 2016). The large compressive force demands may lead to brittle failure of columns and connections. This issue is further investigated by classifying the records into short- and long-period excitations and examining the change in axial force demands of columns under vertical seismic loads for two case studies. The classification of near-fault records gives a deeper perception of the vertical component effects on the seismic response of moment frame buildings.

2 Structural Modeling

The structures under study include five 3-bay special moment-resisting steel frames involving 3–15 stories. Story height and bays width are 3.2 and 6 m, for all cases. Configuration of the frames is presented in Fig. 1. Seismic loading is based on the specifications of Iranian seismic design code (Standard 2800, ver. 4). This standard recommends 0.35 g for base acceleration (A) at the high-seismicity regions. The importance factor of the frames is assumed as 1.0, and the response modification factor (R) is 7.5 for special moment-resisting structures and ultimate capacity design method. Gravity loading and design of structures are accomplished in compliance with specifications of Iranian structure loading code No. 6 (2008) and ANSI/AISC 360-10 (2010) standards. Dead load of 1250 kg/m and live load of 375 kg/m are applied to beam elements as distributed loads. Meanwhile, to take account of the gravity loads transmitted by beams of frames in perpendicular direction, concentrated gravity loads of 6750 and 5175 kg are applied to the middle and corner columns, respectively. Seismic mass per all floors is set to 50 tons (plus the weight of structural elements). The frame members are designed to satisfy the required strength capacity and provide required lateral stiffness to limit the inter-story drift demands to prescribed limits. The sum of moment capacity for columns is greater than that for beams in all of the structural joints. The cross sections are seismically compact to prevent local buckling of members during seismic loadings.

Design sections of sample frames are provided in Table 1.

Incremental nonlinear dynamic analyses are conducted using finite element software SeismoStruct v7.0.4 (2015). This software is essentially utilized for modeling of nonlinear seismic behavior of structural systems subjected to seismic loads. Distributed inelasticity fiber-based frame elements are applied to model frame members. This modeling technique accurately takes account of the axial force and bending moment interaction in columns. Force-based plastic hinge elements (FBPH) are employed for modeling of beams and columns (Scott and Fenvese 2006). Inelastic behavior of FBPH elements is limited to a predefined fraction of elements total length at two ends. This ratio is set to 15%. Second-order geometric nonlinearity is included in time-history analyses. Frame element sections have been divided into 200 fibers extending along the total length of members. Rigid diaphragms are assigned to all floor levels. The Rayleigh damping ratio is set to 2% for first mode and 5% for second mode of vibration. The steel grade ST-37 with yield strength of 240 MPa and elasticity modulus of 210 GPa is used as structural material. A bilinear stress–strain curve with 3% strain-hardening ratio is used to account for material nonlinearity. Beam-to-column connections are assumed to be fully rigid. Also, column bases are fixed to the ground level.

To identify the structural properties of the sample frames, some features of the linear and nonlinear characteristics of the frames are determined using the results of eigenvalue and pushover analyses. The periods and modal mass percentages associated with the three principal modes are obtained for the case study frames. Fundamental period of the structures under study ranges from 0.85 s, for 3-story frame, up to 1.98 s, for 15-story frame. Summarized information is given in Table 2.

3 Ground Motions

Twenty pulse-like records mostly recorded in near distances to fault plus ten far-fault ordinary records are used for nonlinear dynamic analyses. Both the near- and far-fault accelerograms are recorded on soil class C according to the FEMA 356 classification system. The accelerograms

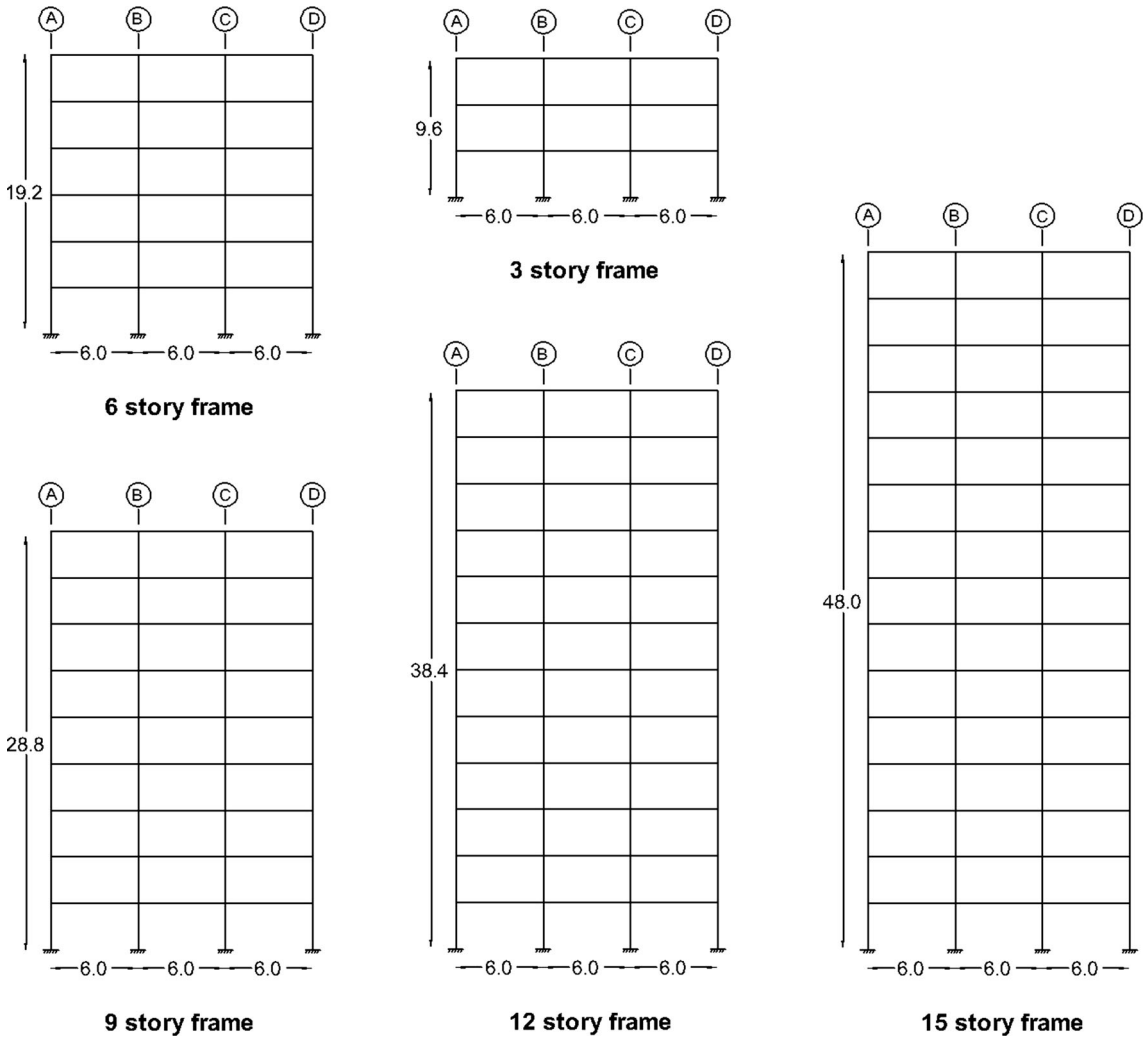

Fig. 1 Geometric dimensions of sample frames

are downloaded from PEER strong motion database Web site. Far-fault records are recorded at far distances to fault and lack impulsive characteristics. The mean period of far-fault records is calculated using the expression proposed by Rathje et al. (2004). This parameter is defined as the weighted mean of the periods for the Fourier amplitude spectrum (FAS) over a predefined frequency range. Mean period of the selected far-fault records extends from 0.37 to 1.29 s with an average of 0.7 s which coincides with the corner period of soil type C.

Near-fault pulse-like records are selected from those having strong velocity pulses in their time history, mainly caused by forward directivity. Baker (2007) proposed three quantitative criteria to identify the pulse-like near-fault records and introduced 92 records satisfying those criteria. Accordingly, a record is considered as near-fault pulse-like motion if: (1) the velocity pulse appears at the beginning of the record, (2) recorded PGV is larger than 30 cm/s, and (3) the pulse index (PI) is larger than 0.85. The near-fault records selected for this study satisfy the mentioned criteria.

A significant portion of the forward directivity ground motion energy is dissipated within short time duration and through high-amplitude waves. Imposing a large amount of energy within a few cycles leads to accumulation of damage in limited parts of the structure. This phenomenon causes brittle behavior which is very destructive to the structural systems (Yang et al. 2010). The pattern of seismic demand distribution is highly dependent on the frequency content of the motion (Sehhat et al. 2011). It has been proved that the pulse period, T_p, appropriately characterizes the frequency content of pulse-like records (Mavroeidis and Papageorgiou 2003). Shahi and Baker (2014) published a paper supported by MATLAB scripts to obtain the pulse period of the earthquake records based on the wavelet transform analysis. This method is employed to obtain the pulse period (T_p) for the selected pulse-like

Table 1 Design sections for sample frames

Frame	Story	Columns in axes A, D	Columns in axes B, C	Beams
15 Story	1–3	Box 360 × 360 × 28	Box 400 × 400 × 30	IPE 550
	4–6	Box 320 × 320 × 25	Box 360 × 360 × 28	IPE 550
	7–10	Box 280 × 280 × 20	Box 340 × 340 × 25	IPE 550
	11	Box 260 × 260 × 2	Box 340 × 340 × 25	IPE 500
	12–13	Box 240 × 240 × 20	Box 320 × 320 × 20	IPE 450
	14–15	Box 220 × 220 × 14.5	Box 240 × 240 × 16	IPE 360
12 Story	1–3	Box 320 × 320 × 25	Box 380 × 380 × 28	IPE 500
	4–5	Box 280 × 280 × 25	Box 340 × 340 × 28	IPE 500
	6	Box 280 × 280 × 25	Box 340 × 340 × 28	IPE 450
	7–8	Box 260 × 260 × 25	Box 320 × 320 × 25	IPE 450
	9	Box 240 × 240 × 16	Box 280 × 280 × 20	IPE 450
	10	Box 240 × 240 × 16	Box 280 × 280 × 20	IPE 400
	11–12	Box 220 × 220 × 12.5	Box 240 × 240 × 14	IPE 360
9 Story	1–3	Box 300 × 300 × 25	Box 360 × 360 × 25	IPE 450
	4–5	Box 260 × 260 × 25	Box 320 × 320 × 25	IPE 450
	6–7	Box 240 × 240 × 20	Box 300 × 300 × 25	IPE 400
	8–9	Box 220 × 220 × 12.5	Box 240 × 240 × 12.5	IPE 360
6 Story	1–2	Box 280 × 280 × 22	Box 320 × 320 × 22	IPE 400
	3–4	Box 260 × 260 × 20	Box 300 × 300 × 20	IPE 400
	5–6	Box 220 × 220 × 14	Box 240 × 240 × 20	IPE 360
3 Story	1–3	Box 220 × 220 × 12	Box 240 × 240 × 16	IPE 360

Table 2 Modal properties of the sample structures

Mode no.		3 Story	6 Story	9 Story	12 Story	15 Story
1	T_1 (s)	0.85	1.24	1.52	1.72	1.98
	MMP (%)	86.7	78.45	75.1	73.17	79.7
2	T_2 (s)	0.27	0.44	0.34	0.68	0.77
	MMP (%)	10.65	11.42	12.27	13.15	12.53
3	T_3 (s)	0.16	0.24	0.225	0.41	0.47
	MMP (%)	2.64	4.94	5.01	5.1	4.98

records. Hence, the near-fault records are classified into two categories:

1. Short-period (SP) records with $t_p < 2$ s.
2. Long-period (LP) records with $t_p > 2$ s.

The ratio of T/T_p is a key parameter to represent the near-fault effects. When this ratio is below unity, the fundamental mode of vibration governs the total seismic response of structure, but when it is greater than unity, the effects of higher modes are more significant. Therefore, the classification of near-fault records elucidates the difference in the near-fault effects in terms of pulse period.

Primary specifications of the near- and far-fault records are presented in Table 3. The ratio of PGV to PGA is given for each record. It is observed that this quantity is averagely larger for ground motions with longer pulse period. This parameter is considered as a measure to quantify the near-fault effects (FEMA P695).

It is remarkable that downloaded near-fault accelerograms are oriented to the direction normal to the fault line, before applying to the model structures.

The magnitude of the considered ground motions ranges from 5 to 7.6. For near-fault records, the closest distance to the fault rupture is mostly below 20 km. However, there are some exceptions that are recorded in farther distances. Far-fault accelerograms lack impulsive features. According to the information presented in Table 3, T_m of near-fault records ranges 1.0–2.0 s which is larger than far-fault records. Average pseudoacceleration response and displacement response spectrums for three sets of records together with design spectrum values are provided in Fig. 2. In this figure, the "Design1" case is referred to design spectrum for far-fault earthquakes and "Design2" case refers to design response spectrum considering near-fault effects. To obtain the spectrums for each record set, first, the response spectrums for each record are calculated

Table 3 Ground motion records

No.	Earthquake	M_w	R (km)	T_p (s)	PGV (cm/s)	PGV/PGA (s^{-1})
(a) Near-fault records						
Set 1, short-period ground motion records, SP						
1	1983 Coalinga-07, Coalinga-14th and Elm (Old CHP)	5.2	7.31	0.4	36	0.05
2	1986 Taiwan SMART1(40), SMART1 M07	6.3	57.6	1.6	36	0.16
3	1986 N. Palm Springs, North Palm Springs	6.1	4.04	1.4	74	0.11
4	1987 Whittier Narrows-01, Downey-Co Maint Bldg	6	20.82	0.8	30	0.13
5	1989 Loma Prieta, Gilroy Array #2	6.9	11.07	1.7	46	0.11
6	2004 Parkfield 02-CA, Fault Zone 9	6	2.85	1.13	24	0.15
7	1995 Kobe, Japan, Takarazuka	6.9	0.27	1	73	0.11
8	1995 Kobe, Japan, Takatori	6.9	1.47	1.6	170	0.25
9	1997 Northwest China-03, Jiashi	6.1	9.98	1.3	37	0.14
10	2000 Yountville, Napa Fire Station #3	5	8.48	0.7	43	0.07
Set 2, long-period ground motion records, LP						
1	1979 Imperial Valley-06, El Centro, Array #3	6.5	0.34	2.4	44	0.13
2	1979 Imperial Valley-06, Agrarias	6.5	0.65	2.3	54	0.18
3	1979 Imperial Valley-06, El Centro Array #5	6.5	3.95	4	91	0.24
4	1979 Imperial Valley-06, El Centro Array #6	6.5	1.35	3.8	112	0.26
5	1981 Westmorland, Parachute Test Site	5.9	16.66	3.6	36	0.22
6	1987 Superstition Hills-02, Parachute Test Site	6.5	0.95	2.3	107	0.26
7	1992 Erzincan, Turkey, Erzincan	6.7	4.38	2.7	95	0.22
8	1994 Northridge-01, Jensen Filter Plant	6.7	5.43	3.5	67	0.13
9	1994 Northridge-01, Jensen Filter Plant Generator	6.7	5.43	3.5	67	0.13
10	1999 Chi–Chi, Taiwan, CHY101	7.6	9.96	4.8	85	0.19

No.	Earthquake	M_W	R (km)	T_m (s)	PGV (cm/s)	PGV/PGA (s^{-1})
(b) Set 3, far-fault records, FF						
1	Chi–Chi CHY101-W, Taiwan, September 20, 1999	7.6	11.14	1.29	70.64	0.2
2	Imperial Valley, H-E01240, October 15, 1979	6.5	10.4	0.75	31.58	0.1
3	Loma Prieta, G02090, October, 1989	6.9	12.7	0.88	40.21	0.13
4	Loma Prieta, G03090, October 18, 1989	6.9	14.4	0.92	44.72	0.12
5	Northridge, CNP 196, January 17, 1994	6.7	15.8	0.8	60.7	0.15
6	Northridge, LOS000, January 17, 1994	6.7	13	0.7	43.1	0.11
7	Tabas, BOS-T1, September 16, 1978	7.4	26.1	0.77	15.44	0.11
8	Kobe, HIK000, January 16, 1995	6.9	95.72	0.9	20.22	0.23
9	N. Palm Springs, TFS000, July 8, 1986	6.06	64.8	0.37	6.9	0.06
10	Manjil 1990, BHRC Rudsar	7.37	64.67	0.69	11.54	0.12

through solving the motion equations for SDOF systems with different periods, assuming 5% viscous damping. Then the average spectrum is calculated by averaging the spectrum ordinates for records belonging to each set.

In this paper, sets 1, 2 and 3 refer to SP, LP and FF record sets, respectively. Comparison of response spectrums reveals that application of N factor appropriately accounts for the effects of near-fault ground motions on elastic response of single-degree-of-freedom systems. However, the findings of previous researches have shown that the damaging potential of pulse-like records may not be fully accounted by this method (Baker and Cornell 2008). In addition, it is evident that the acceleration response spectrum of short-period records is lower than other ground motion sets, in medium- to long-period range. In other words, the damaging potential of near-fault effects is associated with the records with relatively long pulse period.

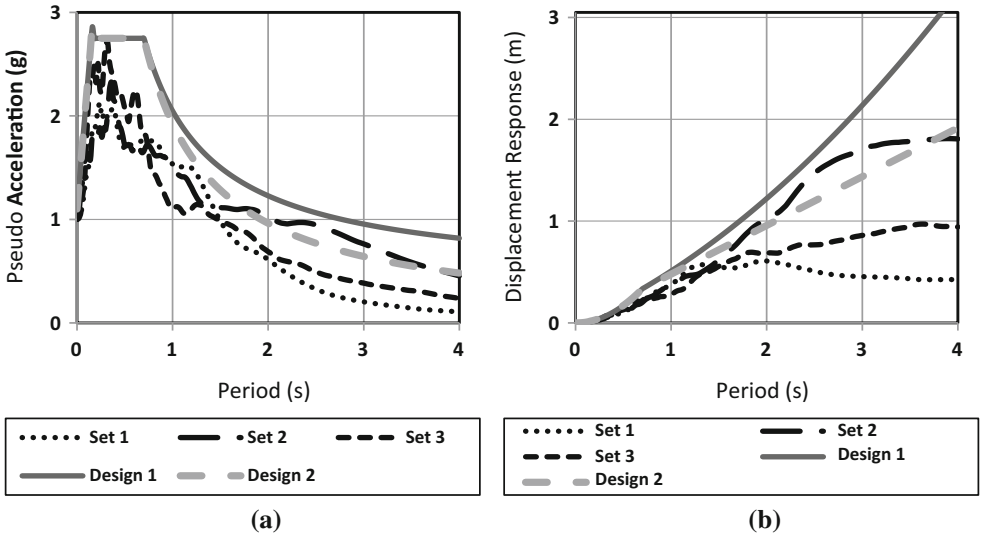

Fig. 2 Response spectrum of ground motion sets, **a** pseudoacceleration response, **b** displacement response

4 Methodology

Incremental dynamic analysis is utilized to identify the seismic behavior of the sample structures subjected to ground motion excitations with different intensities. Maximum roof drift ratio and maximum base shear are adopted as global response quantities to measure the damaging potential of different ground motions. The focus of the study is on the design-basis earthquakes. According to the implications of the Iranian seismic code for high-seismicity regions, the base acceleration (A) for design-basis earthquake (DBE) is assumed to be 0.35 g. In addition, it is assumed that base acceleration for maximum considered earthquake (MCE) is $1.5 \times 0.35 = 0.53$ g. This assumption is approximate, but consideration of earthquake intensity more severe than DBE hazard level would reveal the seismic response of structures for highly nonlinear states.

In addition to the mentioned intensities, other scale factors are used in IDA analyses (equivalent to PGA of 0.05 g to larger than 1 g). However, the major parts of the study are based on the DBE and MCE hazard levels; comparison of pushover and IDA curves is presented to monitor the difference of two methods and investigate the effect of different ground motion types in wider intensity range.

The current study focuses on the influence of ground motion characteristics on two parameters:

1. Base shear and roof drift demands.
2. Variation of story shear demands.

Meanwhile, the accuracy of linear and nonlinear static procedures to assess the seismic demand of moment-resisting frames is examined. In the last part of the study, the amount of increase in column axial forces due to vertical component of near-fault seismic excitations is investigated.

4.1 Global Seismic Demands

The average of peak roof drift ratio and maximum base shear demand of the steel moment frames subjected to ground motions scaled to PGA of 0.35 g is provided in Fig. 3. In this manner, the individual records are scaled to reach the prescribed peak ground acceleration. This method of scaling is a suitable approach for the comparison of ground motions in terms of frequency characteristics.

Considering the bar charts presented in Fig. 3, the LP records tend to impose larger demands on almost all of the sample frames. With the increase in the frame height, the effect of LP records gets greater. This is due to the fact that the increase in height leads to larger periods. In elastic state, when ratio of T/T_p gets near to unity, the damaging potential of the near-fault records tends to grow (Sehhati et al. 2011). In severe earthquakes, the nonlinear behavior leads to period elongation. Therefore, the larger pulse period will impose more significant responses. It is notable that the roof drift response is more sensitive to ground motion frequency content compared to base shear demand. In fact, when the seismic response enters the nonlinear phase, the displacements grow more rapidly than base shear response. For example, the average peak base shear of 15-story frame for SP, LP and FF records equals to 0.118, 0.147 and 0.131 W, respectively, which offers less than 15% increase in maximum base shear demand for LP records compared to ordinary FF records. The average roof drift demand for SP, LP and FF records corresponds to 0.67, 0.96 and 0.71%, respectively. Therefore, the displacement response of the 15-story frame is approximately

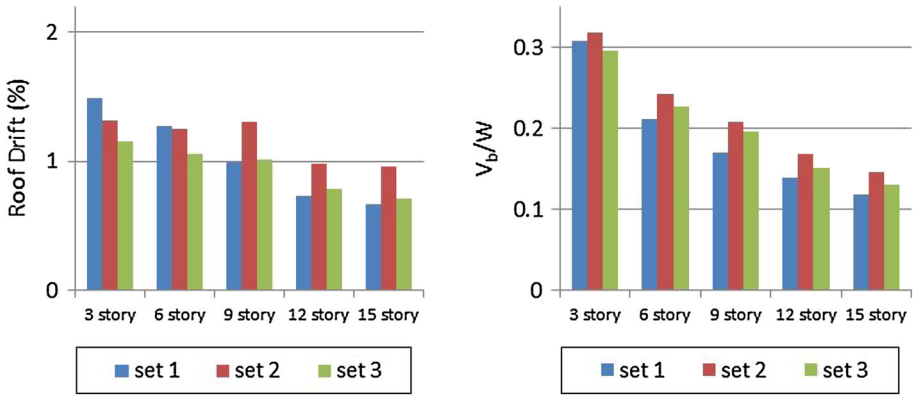

Fig. 3 Peak global seismic demands for PGA of 0.35 g

35% larger for LP ground motions compared to FF motions. The SP near-fault records impose lower drifts compared with other types of excitations. In low-rise frames, both the LP and SP excitations induce greater demands compared to FF records. However, the difference among the ground motion sets is less tangible for low-rise frames.

As stated in Sect. 3, Iranian seismic code considers the near-fault effects through amplification of design spectrum ordinates by N factor. This factor represents the difference between seismic response parameters for near- and far-fault motions and linearly increases the seismic demands for design of structures. For the sample structures of the present study the N factor ranges from 1 for 3-story frame to 1.24 for 15-story frame. On the basis of the results of this study, application of N factor may not adequately capture the near-fault effects on the displacement response of structures. This is in agreement with the findings of Gerami and Abdollahzadeh which predict near-fault motions may induce 1.5–2.5 times larger displacements in comparison with far-fault ordinary motions.

In addition, the estimation of base shear demand does not require a modification factor as large as N factor. In other words, the application of N factor leads to overestimation of force demands for design of frame members in current design approaches. Moreover, the linear correlation between the N factor and fundamental period (T) is not detected. Estimated values for N factor of the sample frames together with those obtained from Eq. (6) are provided in Table 4. N factors associated with each demand parameter are simply estimated by dividing the average response for near-fault motions to that of far-fault records. It should be emphasized that the application scope of the current study is limited to regular steel moment frames with similar specifications to the case study structures.

The difference in the N factor obtained from analyses of the current study with the Iranian seismic code suggestion is due to the fact that the essence of the spectral modification method is the elastic response of the SDOF systems. This may not account for the actual nonlinear behavior of structures when subjected to moderate to severe earthquake loads (Cornell and Baker 2008). For this reason, some researchers have suggested to modify the behavior factor in addition to spectral modification to completely capture the severe damaging potential of pulse-like motions (Soltangharaei et al. 2016).

To find out whether the consideration of elastic response spectrum ordinates captures the damaging potential of pulse-like records, the ground motions are scaled to reach the same target spectral acceleration. The design spectrum is calculated for each sample frame, and the scale factor of each record is computed using the following expression:

$$SF_i = \frac{S_a(T_1)}{AB} \tag{6}$$

where A is base acceleration which is 0.35 g, B is normalized design spectrum, and $S_a(T_1)$ is the spectral acceleration corresponding to fundamental period of vibration for individual records. Seismic demands of the sample

Table 4 Estimation of spectrum modification factor

Frame	Experimental period (s)	N factor		
		Equation (6)	Base shear	Roof drift
3 Story	0.55	1	1.15	1.07
6 Story	0.92	1.05	1.19	1.07
9 Story	1.24	1.12	1.29	1.07
12 Story	1.54	1.18	1.25	1.12
15 Story	1.82	1.24	1.34	1.12

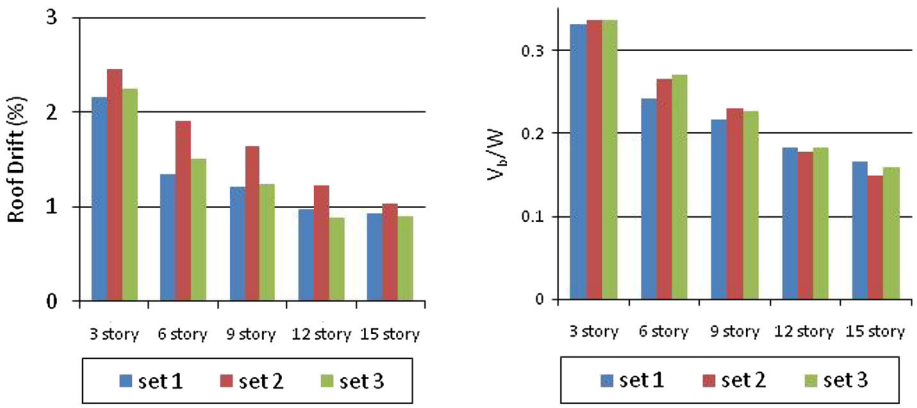

Fig. 4 Peak seismic demands for scaled ground motions

frames subjected to scaled ground motions are presented in Fig. 4.

Comparison of seismic demands of the sample frames reveals that incorporation of response spectrum corresponding to the fundamental period of vibration may not completely account for the damaging potential of LP ground motions. However, it reduces the difference among the FF and SP records. Generally, LP ground motions tend to impose 10–35% larger drifts compared to SP and FF ground motions. For maximum base shear demand, the difference among the record sets is not significant. The ratio of maximum base shear associated with LP records to FF or SP records fluctuates in 0.9–1.1 range. Hence, shear demand estimation of moment frames mainly depends on the spectral acceleration of the ground motion with limited influence of impulsive feature of the near-fault pulse-like earthquakes. In other words, impulsive feature of near-fault records has little effect on base shear demand of steel moment frames.

Scaling method influences the results of time-history analyses. Iranian seismic code suggests that accelerograms are scaled in such a manner that the average acceleration response spectrum not be less than 90% of the design spectrum within the range of $0.2T$–$1.5T$ periods, where T is the fundamental period of vibration. This method attempts to account for the spectral shape of the records. To examine the preciseness of this approach, the records are scaled in this manner. The maximum base shear and peak roof drifts for the three sets of records obtained through this method are provided in Fig. 5.

Comparison of the roof drifts induced by different ground motion sets reveals that this methodology is not able to take account of the near-fault effects on the seismic demands of the structures. Inefficiency of this scaling approach is because the spectral characteristics of individual records are not directly considered. Moreover, the impulsive characteristics of near-fault motions must be thoroughly considered.

4.2 Base Shear Modification Factor

The actual base shear experienced by the supports of structure is considerably larger than design base shear. This is mainly due to the overall over-strength and higher-mode effects. Seismic codes suggest that the design base shear is multiplied by an amplification factor to calculate the actual base shear. The actual peak shear demand is used to control the brittle collapse of some structural elements, e.g., columns under axial loads. Iranian seismic design code suggests a value of 3 as amplification factor for special steel moment-resisting frame buildings. Conventionally, pushover method has been employed to evaluate this parameter (Gerami et al. 2016). Accordingly, the base shear amplification factor is defined as the ratio of maximum base shear (V_u) to the design base shear (which is expected to be equivalent to base shear at the first yield in the structure). Due to the fact that conventional pushover procedures are not able to capture the higher-mode effects, the maximum base shear obtained by this method may be underestimated. In addition, to control the story drift demands to not exceed the prescribed limits, design cross sections are larger than what strength-based specifications require, particularly for steel moment frames. Therefore, the design base shear is generally lower than base shear at the first yield. Application of large cross sections increases the strength capacity of the members, but the larger force demands may lead to transmission of unexpectedly large actions to the adjoining members.

In this part of the study, base shear amplification factor is evaluated and compared for two different methods. In the first method, the pushover analysis with lateral load pattern corresponding to first mode of vibration is employed to estimate the maximum shear demand and in the second method the IDA approach is utilized for this purpose. Base shear modification is evaluated by dividing the maximum base shear to design-based value. This method does not include the effect of material over-strength. To account for the material over-strength, the

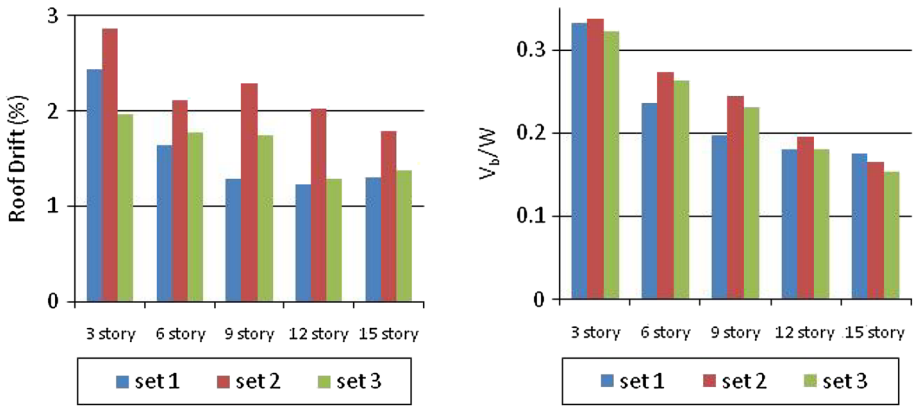

Fig. 5 Peak seismic demands for standard-based scaled ground motions

amplification factor must be multiplied by a factor of about 1.25 (Izadinia et al. 2012). The estimated amplification factors through pushover analyses are presented in Table 5. The results of pushover analysis are consistent with the amplification factor proposed by Iranian seismic design code.

Regarding the fact that static procedures (e.g., pushover analysis) may not sufficiently capture the dynamic features of structural behavior against seismic loads, in the second method the maximum base shear demands obtained from time-history analyses are used to specify shear force amplification factor. Based on the results, the difference among various types of ground motion records is negligible. However, for high-rise frames, LP records tend to impose up to 10% larger shear demands in comparison with other ground motion classes. To evaluate the shear force amplification factor, each ground motion record is scaled to reach design response spectrum using Eq. (6). The maximum of base shear demands during dynamic loading step is selected as V_{max} for that case. The amplification factors derived by this method are given in Table 6. It is observed that time-history analysis results in larger factors compared with pushover analysis. This is mainly due to higher-mode effects. In other words, pushover analysis predicts relatively uniform distribution of plasticity within the structural elements, while the dynamic analysis gives different patterns of plasticity distribution depending on the ground motion characteristics and structural properties.

To illustrate the effect of analysis method in estimation of shear demands and compare the effects of different ground motion types, variation of base shear versus roof drift ratio obtained from IDA and pushover analyses is provided in Fig. 6. The average curves for each ground motion set together with the curves derived from pushover analyses with three different lateral load patterns are provided for the sample frames. IDA plot of each set is derived by averaging the IDA curves for the associated records. It can be found that for equal roof displacement, pushover analysis yields lower values for base shear demand. This means that the force demand of members will be underestimated by pushover analysis. Moreover, the SP records induce larger base shear for the same roof drift demand. Generally, short-period ground motions tend to excite higher modes leading to high ratios of shear demand to roof drift ratio.

The increase in frame height causes larger difference among record types which is due to augmentation of higher-mode participation in taller structures.

Implementation of conventional pushover procedures requires the assumption of a pattern for lateral force distribution. Seismic design code suggests different patterns for lateral force distribution from which inverse triangle distribution (also called linear distribution), force distribution based on the essential mode shape of the structure and load distribution proportional to story mass are the most frequent types which are examined in this study.

The comparison of pushover curves for different load patterns indicates that for higher frames, the mass-

Table 5 Base shear amplification factor obtained from pushover analyses

Sample frame	S_a (g)	W (ton)	V_{Design} (kN)	V_{max} (kN)	$\Omega = V_{max}/V_d$
3 Story	2.33	177.75	190	509	2.68
6 Story	1.73	344.8	273	748	2.74
9 Story	1.49	490	334	896	2.68
12 Story	1.34	736.8	371	1040	2.80
15 Story	1.24	1041.2	539	1600	2.97

Table 6 Base shear amplification factor obtained from time-history analyses

Sample frame	S_a (g)	W (ton)	V_{Design} (kN)	V_{max} (kN)	$\Omega = V_{max}/V_d$
3 Story	2.33	177.75	190	578	3.04
6 Story	1.73	344.8	273	872	3.19
9 Story	1.49	490	334	1080	3.23
12 Story	1.34	736.8	371	1346	3.63
15 Story	1.24	1041.2	539	1683	3.12

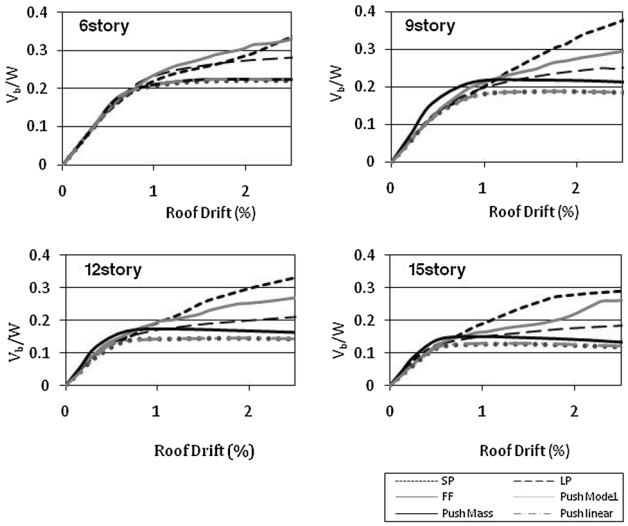

Fig. 6 Base shear versus roof drift ratio curves

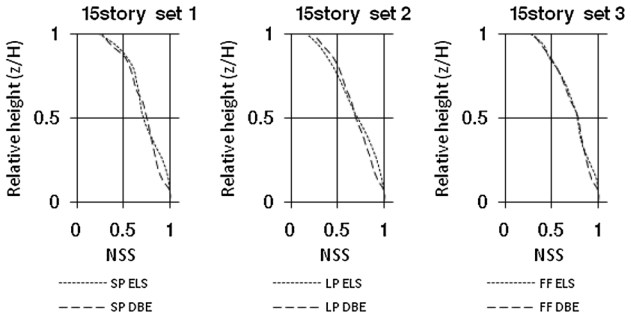

Fig. 7 Distribution of normalized story shears, NSS, for 15-story frame

proportioned load pattern yields greater V_{max}. This means that over-strength estimations provided in Table 5 would be greater for mass-proportioned load pattern.

4.3 Shear Force Distribution Pattern

Precise estimation of shear force demand distribution over the height of the structures can greatly improve the accuracy of strength demand prediction of structural members and reduce the approximations for global instability calculations. Regarding the fact that the lateral stiffness of stories changes when the structure response enters in nonlinear state, it may affect the shear demand distribution. Moreover, frequency content of ground motions influences the distribution of seismic demands. In this part of the study, aforementioned issues as well as the accuracy of linear procedures to estimate the pattern of story shears are investigated.

4.3.1 Shear Distribution in Linear and Nonlinear States

Distribution of normalized story shears (NSS) along the height of 15-story frame associated with linear and nonlinear responses is compared in Fig. 7. The plots are separately given for each ground motion set. It is assumed that seismic response of the sample frames for PGA of 0.05 g is essentially elastic. To determine the seismic demands for nonlinear state, ground motion time histories are scaled according to Eq. (6). Story shear demands are computed by the summation of column shear forces at each story level. Then, the NSS values are computed through division of story shears by base shear demand. It is observed that the nonlinear behavior has negligible effect on the seismic shear distribution. However, the shear demands tend to move toward upper stories for nonlinear response associated with DBE ground motions. This is more tangible for LP records which cause severe nonlinearity compared to other records. In highly nonlinear states, plastic deformations concentrate in lower stories causing the reduction in story lateral stiffness. Thus, shear demands transfer toward upper parts of structure.

4.3.2 Effect of Frequency Content on Shear Distribution

The frequency content of ground motion records may influence the shear distribution pattern. Static analysis methods, including linear and nonlinear procedures, assume the same pattern of lateral force for all types of ground motions. In this part of the study, the effect of ground motion type on shear distribution pattern is investigated. In addition, the accuracy of static procedures is examined.

Distributions of shear forces for 6-, 9- and 15-story frames are illustrated in Figs. 8, 9 and 10, respectively. The analytical methods included in comparative studies consist of eight different cases in three groups: (1) pseudostatic analysis with three different lateral force patterns (Eqs. (3), (4) and first mode), (2) pushover analysis with three different load patterns (triangular, mass proportionate and first mode) and (3) time-history analysis for three sets of records (SP, LP and FF). Comparison of results indicates that pushover analysis with triangular load pattern yields very similar results to first-mode load pattern. Therefore, the triangular load pattern is not presented in the figures. It is remarkable that the charts are given for DBE hazard level. Evidently, the pattern of story shear distribution is more important for higher frames. Because the peak shear demands are normalized to base shear, the difference in first story shear is zero for all analysis approaches. The actual shear demand of each story is estimated using Eq. (7).

$$V_{i,u} = \alpha_i \Omega V_{i,d} \tag{7}$$

where $V_{i,u}$ is the actual shear demand for ith story, α_i is the NSS modification factor of ith story for a given analytical method which calibrates the shear distribution vector, Ω is base shear amplification factor, and $V_{i,d}$ is the story shear obtained from static analysis using design base shear.

According to the results of nonlinear dynamic analyses, pushover analysis with mass proportionate load pattern reveals very unreliable results for story shears. It is recommended to not apply this analytical approach to estimate shear demands. Static procedures generally underestimate shear demands for upper stories. The amount of inaccuracy depends on the load pattern and the ground motion type under consideration. The trend shown in Figs. 8, 9 and 10 is similarly repeated for 3- and 12-story case studies.

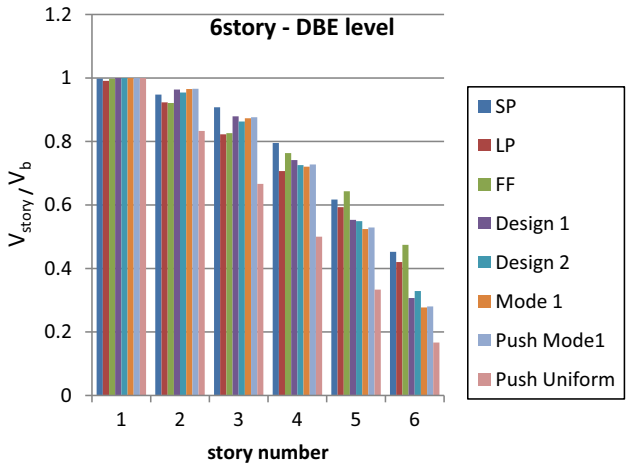

Fig. 8 Distribution of NSS along the height of 6-story frame

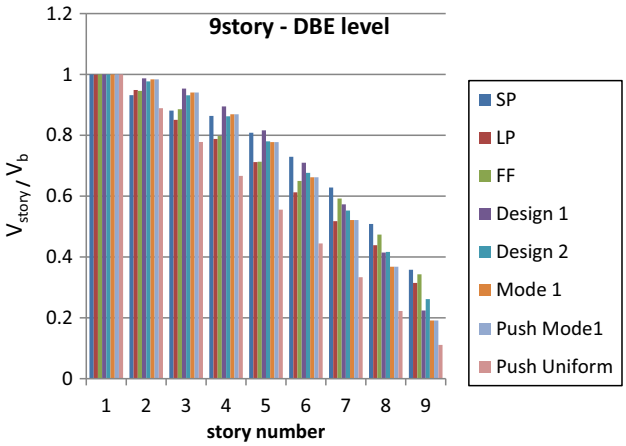

Fig. 9 Distribution of NSS along the height of 9-story frame

The results of pushover procedures to estimate shear distribution pattern are even less reliable than linear static procedures. Regarding the fact that the aim of pushover analysis is to obtain conservative results, the modification of shear demands is inevitable. Regarding the effect of ground motion class, LP records tend to transfer shear demands toward lower stories compared to FF and SP records. In general, the long-period records tend to excite first mode of vibration and transfer seismic demands to lower stories.

For almost all the sample structures, α factor must be applied to stories located at upper one-third stories, except for 6-story frame in which the fourth story must be included. The α factor is estimated for static procedures by dividing the average NSS obtained from nonlinear time-history analyses to those obtained from static procedures. Since the mass proportionate load pattern gives highly approximate results and the triangular load pattern yields the same results as first-mode load pattern, only first-mode pushover case is incorporated in α calculations. It is again emphasized that the $\alpha < 1$ can be replaced with 1 as a conservative measure. Estimated α factors for 6-, 9- and 15-story frames are presented in Tables 7, 8 and 9, respectively.

It can be observed that α factor may reach to 2.5 for top story. This conclusion is compatible with the results of other researchers for far-fault ground motions (Kumar et al. 2013). Generally, an increase in height leads to larger α factor. Comparison of static linear procedures demonstrates that Eq. (3) is more efficient than other lateral load patterns when the story shear demands are under consideration. Also, the NSS amplification factor generally gets larger for taller frames. This is due to participation of higher modes which is more prominent for larger structures.

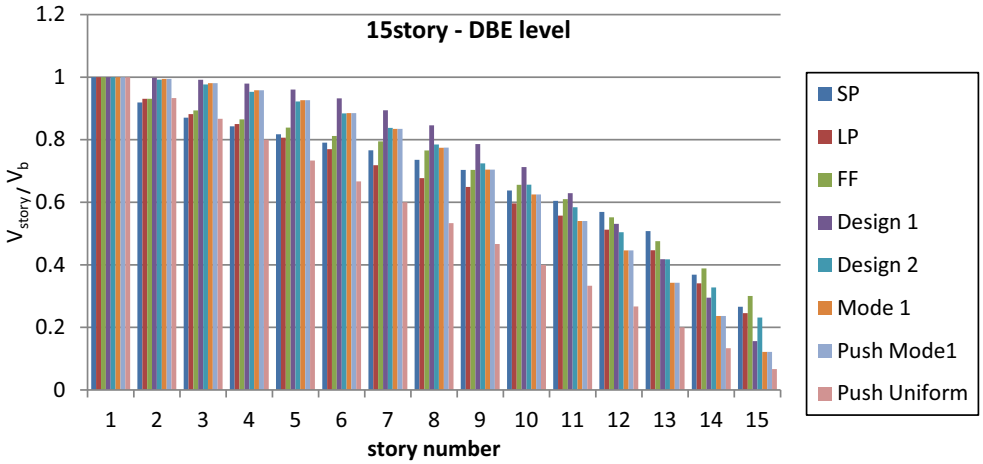

Fig. 10 Distribution of NSS along the height of 15-story frame

4.4 Effect of Vertical Excitations

One of the most prominent aspects of near-fault ground motions is the large vertical acceleration. Among others, vertical accelerations may cause brittle behavior within column members (Dana et al. 2014). This phenomenon together with impulsive feature of long-period pulse-like excitations leads to severe damage to the constructions (Sultana and Youssef 2016). In this part of the study, the increase in column axial forces due to the application of vertical component of accelerograms is quantified for 6- and 12-story sample frames. For this purpose, the vertical component of the records is scaled in such a way that the ratio of horizontal to vertical acceleration remains constant for each record. The axial forces are evaluated through simultaneous application of horizontal and vertical accelerations to the base points.

The investigations revealed that the influence of vertical excitations on middle and corner columns is approximately the same. Thus, the results are presented only for middle columns. For each story level, the maximum compressive force of two middle columns is considered as the representative column force. The variation of column forces along the height of 6-story and 12-story frames is depicted in Figs. 11 and 12, respectively. It is observed that for LP records, application of vertical accelerations increases the peak column forces by up to 100%. For SP records, the increase in column axial forces reaches to 30%. This finding is in agreement with prediction of 80% increase in column forces stated in Sultana and Youssef (2016). The amplification of column forces is more pronounced for upper stories. This effect may lead to brittle behavior in columns and must be considered within the design of column members. In addition, the increase in vertical loads is crucial for instability control of structures against seismic loads.

It is emphasized that for moderate earthquakes, application of vertical excitations has a negligible effect on the drift demands. However, for severe earthquakes where columns undergo large p-delta actions, vertical seismic loads cause brittle buckling of columns. This effect may lead to structural instability followed by large displacements. Therefore, the columns must be able to resist the axial forces induced by gravity and earthquake loads.

5 Conclusions

In this study, the effect of near-fault ground motions on the global response and seismic shear demands of steel moment-resisting frames is investigated. In addition, the accuracy of static procedures to predict the shear demands is examined. Nonlinear time-history analyses as well as static linear and nonlinear procedures with different load patterns were conducted to assess the seismic response of five sample steel moment-resisting frames with 3–15 stories. The results of study are summarized as follows:

1. Long-period pulse-like ground motions tend to impose up to 35% larger global drift in comparison with far-fault ground motions with the same peak ground acceleration, but they do not necessarily impose larger base shear demands.
2. Scaling ground motion records either based on the spectral acceleration corresponding to first mode of vibration or based on the scaling methodology proposed by Iranian seismic design code (or other similar standards) do not capture the damaging potential of near-fault ground motions.
3. The base shear amplification factor is estimated 3 by pushover analysis and 3.5 using time-history analysis.

Table 7 α Factor of static procedures for different ground motion sets (6-story frame)

Story	SP ground motions				LP ground motions				FF ground motions			
	Equation 4	Equation 3	Mode 1	Pushover	Equation 4	Equation 3	Mode 1	Pushover	Equation 4	Equation 3	Mode 1	Pushover
4	1.07	1.10	1.10	1.09	0.95	0.97	0.98	0.97	1.03	1.05	1.06	1.05
5	1.12	1.12	1.18	1.17	1.07	1.08	1.13	1.12	1.16	1.17	1.23	1.22
6	1.47	1.38	1.63	1.61	1.37	1.28	1.52	1.50	1.55	1.44	1.71	1.69

Table 8 α Factor of static procedures for different ground motion sets (9-story frame)

Story	SP ground motions				LP ground motions				FF ground motions			
	Equation 4	Equation 3	Mode 1	Pushover	Equation 4	Equation 3	Mode 1	Pushover	Equation 4	Equation 3	Mode 1	Pushover
7	1.10	1.14	1.21	1.21	0.90	0.94	0.99	0.99	1.03	1.07	1.14	1.14
8	1.23	1.22	1.38	1.38	1.06	1.05	1.19	1.19	1.14	1.14	1.29	1.29
9	1.60	1.37	1.87	1.87	1.41	1.20	1.65	1.65	1.53	1.31	1.79	1.79

Table 9 α Factor of static procedures for different ground motion sets (15-story frame)

Story	SP ground motions				LP ground motions				FF ground motions			
	Equation 4	Equation 3	Mode 1	Pushover	Equation 4	Equation 3	Mode 1	Pushover	Equation 4	Equation 3	Mode 1	Pushover
11	0.96	1.03	1.12	1.12	0.89	0.95	1.03	1.03	0.97	1.04	1.13	1.13
12	1.07	1.13	1.28	1.27	0.96	1.02	1.15	1.15	1.04	1.09	1.24	1.24
13	1.22	1.22	1.48	1.48	1.07	1.07	1.30	1.30	1.14	1.14	1.39	1.39
14	1.25	1.12	1.56	1.56	1.15	1.04	1.44	1.44	1.32	1.18	1.64	1.64
15	1.70	1.15	2.19	2.19	1.57	1.06	2.02	2.02	1.93	1.30	2.47	2.47

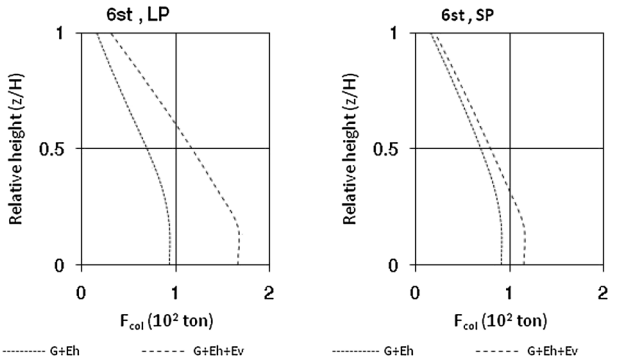

Fig. 11 Variation of peak column axial forces along the height of 6-story frame

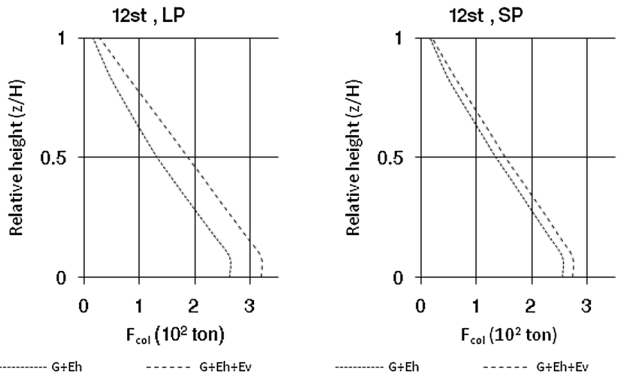

Fig. 12 Variation of peak column axial forces along the height of 12-story frame

4. Static analysis procedures highly underestimate the story shear demands in stories located at the upper one-third of the steel frame structures. To address this issue, a modification factor is introduced which reaches up to 2.5 for top story shear demand estimation.
5. The upper stories share less portion of total shear when subjected to LP records, compared with far-fault and short-period ground motions.
6. In comparison with lateral force pattern proportionate to first mode of vibration or the expression given in fourth edition of Iranian seismic design code, the lateral load pattern proposed in third edition of this code, which allocates a fraction of base shear to the roof level, is more accurate for assessment of shear demands.
7. Application of vertical component of near-fault earthquake excitations increases the column axial forces which may lead to brittle collapse of columns. The average amount of increase is 30% for short-period and 100% for long-period records.

Regarding the fact that inductile behavior of structural elements under unpredicted strength demands may lead to severe damage to the buildings located at the high-seismicity regions, it is recommended to improve the predictive expressions for strength demands of constructions prone to near-fault pulse-like motions.

References

ANSI/AISC 360-10 (2010) Specification for structural steel buildings. American Institute of Steel Construction, Chicago

ASCE standard 07–10 (2010) Minimum design loads for buildings and other structures. American Society of Civil Engineers, Reston

ASCE/SEI 41-13 (2014) Seismic rehabilitation of existing buildings. American Society of Civil Engineers, Reston

Baker JW (2007) Quantitative classification of near-fault ground motions. Bull Seismol Soc Am 97(5):1486–1501

Baker JW, Cornell CA (2008) Vector-valued intensity measures for pulse-like near-fault ground motions. Eng Struct 30:1048–1057

CEN. Eurocode 8 (2004) Design of structures for earthquake resistance—part 1: general rules, seismic actions and rules for buildings. EN 1998-1. European Committee of standardization, Brussels

Dana M et al (2014) Effects of the seismic vertical component on structural behavior—an analytical study of current code practices and potential areas of improvement. In: Tenth U.S. national conference on earthquake engineering. Frontiers of earthquake engineering. Anchorage, Alaska

FEMA 356 Prestandard and commentary for the seismic rehabilitation of buildings. Reston

FEMA P695 (2009) Qualification of building seismic performance factors. Federal Emergency Management Agency, Washington

Gerami M, Abdollahzadeh D (2015) Vulnerability of steel moment-resisting frames under effects of forward directivity. Struct Design Tall Spec 24:97–122

Gerami M, Mashayekhi AH, Siahpolo N (2016) Computation of R factor for steel moment frames by using conventional and adaptive pushover methods. Arab J Sci Eng. https://doi.org/10.1007/s13369-016-2257-5

Iranian Code of Practice for Seismic Resistant Design of Buildings (2005) Standard No. 2800, 3rd edn. Building &Housing Research Center, Tehran

Iranian National Building Regulations (2008) Loads on buildings, Code No. 6. Iran National Building Regulations Centre, INBR Publications, Tehran

Iranian Code of Practice for Seismic Resistant Design of Buildings (2015) Standard No. 2800, 4th edn. Building &Housing Research Center, Tehran

Izadiniaa M, Rahgozar M, Mohammadrezaei O (2012) Response modification factor for steel moment-resisting frames by different pushover analysis methods. J Constr Steel Res 79:83–90

Kumar M, Stafford PJ, Elghazouli AY (2013) Seismic shear demands in multi-storey steel frames designed to Eurocode 8. Eng Struct 52:69–87

Mavroeidis GP, Papageorgiou AS (2003) A mathematical representation of near-fault ground motions. Bull Seismol Soc Am 93(3):1099–1131

Medina AR, Krawinkler HJ (2005) Strength demand issues relevant for the seismic design of moment-resisting frames. Earthq Spectra 21:415

Pettinga JD, Priestley MJN (2005) Dynamic behaviour of reinforced concrete frames designed with direct displacement-based design. J Earthq Eng 9(2):309–330

Rathje EM, Faraj F, Russel S, Bray JD (2004) Empirical relationships for frequency content parameters of earthquake ground motions. Earthq Spectra 20(1):119–144

Scott MH, Fenvese GL (2006) Plastic hinge integration method for force-based beam-column elements. ASCE J Struct Eng 132(2):244–252

Sehhati R, Rodriguez-Marek A, ElGawady M, William F (2011) Effects of near-fault ground motions and equivalent pulses on multi-story structures. Eng Struct 33:767–779

SeismoStruct (2015) A computer program for static and dynamic analysis for framed structures. Version 7.0.4. URL:www.seismosoft.com (online)

Shahi SK, Baker JW (2014) An efficient algorithm to identify strong-velocity pulses in multicomponent ground motions. Bull Seismol Soc Am 104(5):2456–2466

Soltangharaei V, Razi M, Gerami M (2016) Comparative evaluation of behavior factor of SMRF structures for near and far fault ground motions. Periodica Polytechnica. Civil Engineering, 60(1):75–82

Sultana P, Youssef MA (2016) Prediction of local seismic damage in steel moment resisting frames. J Constr Steel Res 122:122–137

Yang D, Pan JW, Lin G (2010) Interstory drift ratio of building structures subjected to near-fault ground motions based on generalized drift spectral analysis. Soil Dyn Earthq Eng 30:1182–1197